ER-4949

RESEARCH ON THE
VORTEX MHD POWER GENERATOR

FIRST QUARTERLY PROGRESS REPORT

W. C. Davis, E. L. Krasnoff, and W. F. Wade   JULY 1962

TAPCO

A Division of

Thompson Ramo Wooldridge, Inc., Cleveland, Ohio

8731002

(NASA Contract No. NAS3-2526; TRW Proj. 512-009604-08)

RQT-7385

TAPCO

A Division of

Thompson Ramo Wooldridge Inc.

SUBJECT: FIRST QUARTERLY PROGRESS REPORT, JULY 1962

CONTRACT NO.:   NASA NAS5-2526

TRW PROJECT NO.: 512-009604-08

TITLE: RESEARCH ON THE VORTEX MHD POWER GENERATOR

W C Davis
W. C. Davis
Engineering Specialist

R. T. Craig
Project Manager

1 INTRODUCTION

This report summarizes the efforts during the first quarter of a one year research program, whose principal objective is the demonstration of feasibility and advancement of the vortex MHD power generator concept. The research is essentially a continuation of the investigation initiated under NASA Contract No. NAS5-705.

Experimental efforts have concentrated on the following: (a) design and fabrication of an advanced experimental model of a vortex MHD generator; (b) visualization study of the flow in an incompressible vortex; and (c) design of a vortex chamber for detailed study of the velocity field in a compressible vortex.

The supporting theoretical research included a preliminary study of the application of turbulent boundary layer correlation to vortex flow, including the region adjacent to a central body in the vortex.

II SUMMARY

Facilities were established which will enable the operation of dual arc jets simultaneously for the testing of multiple jet vortex MHD generators.

A new and more sophisticated experimental model of the vortex MHD generator was designed and is being fabricated. It incorporates the changes and refinements suggested by the NAS5-703 research.

Visualization studies, utilizing tufts and ink injection, were conducted in an incompressible vortex. The limiting conditions (Reynolds number) for laminar vortex flow were observed. Other phenomena studied included the distrubances in the slip plane between the driving jet and the vortex flow field, and the flow in the region of a slotted center body cylinder.

A vortex chamber was designed which will facilitate a detailed study of the velocity field in a compressible vortex.

Preliminary application of a pseudo-laminar type of boundary layer analysis was successfully employed for the description of turbulent flow profiles in a vortex which also contains a porous center body.
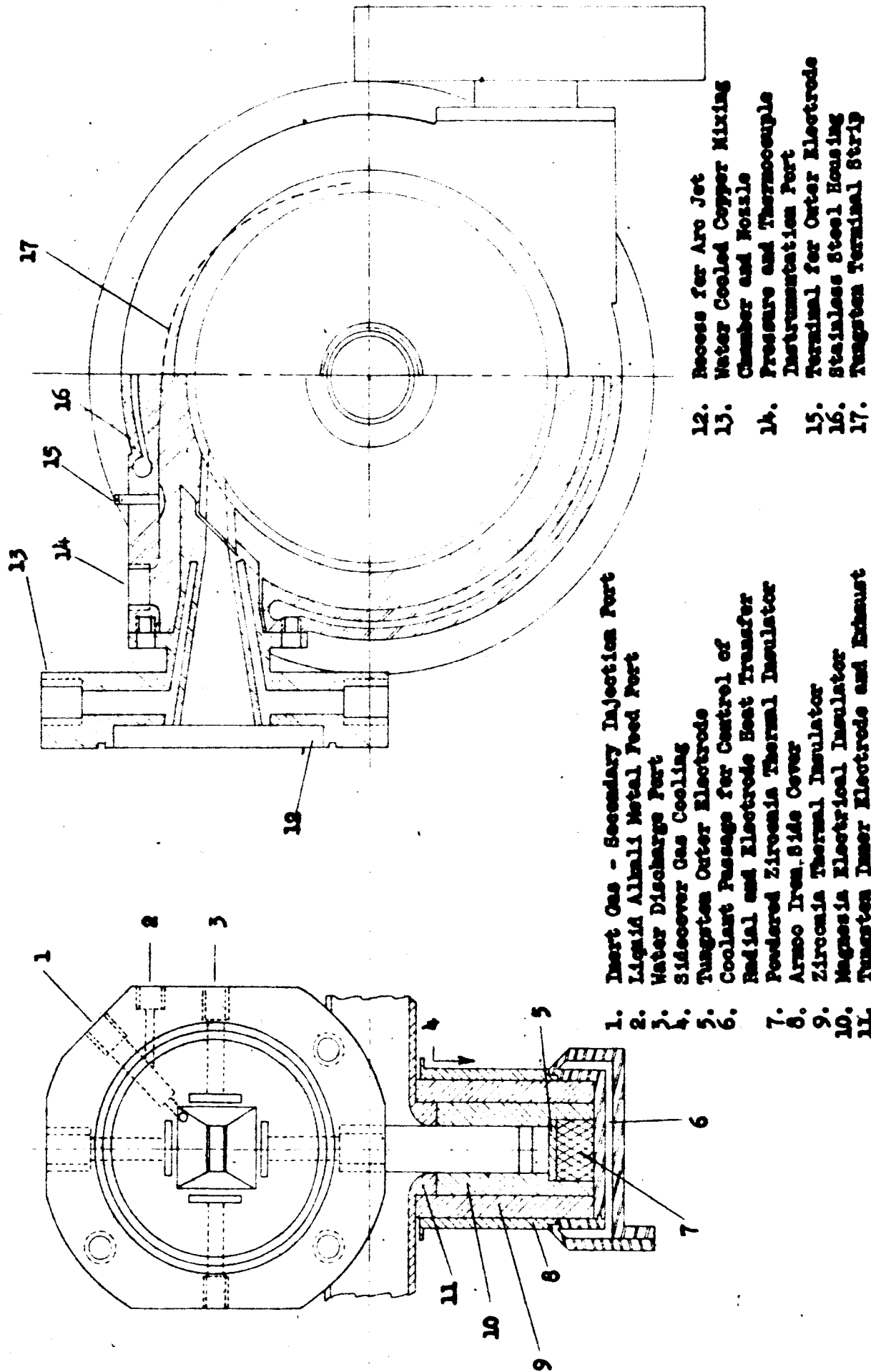
III ITEMS OF PROGRESS

1. Vortex MHD Generator Experiments

Vortex Generator Design and Facility. Based on the recommendations
of the preceeding NAS5-703 contract, the initial efforts on the current
vortex generator program commenced with the acquisition and installation
of a dual arc jet facility. The arc jets are identical Plasmadyne M-4
subsonic heads coupled to two power supplies (each rated at 40 KW con-
tinuous, 60 KW peak) for separate or simultaneous operation. It is ex-
pected that simultaneous operation of both arc jets will provide a factor
of four increase in the plasma mass flow capability as compared with pre-
vious operation. Thus, the increased flow rate, approximately 25 gm sec^{-1}
of seeded argon, will minimize the relative importance of the auxiliary
phenomena which were encountered in the earlier program. The effects
associated with single and multiple jet-driven vortices previously in-
vestigated only in cold gas experiments now can be studied in hot gas
power generation experiments.

The design of a new and more sophisticated vortex MHD generator was
completed and the unit now is being fabricated. It incorporates the
changes and refinements suggested by the NAS5-703 research. Also in-
cluded are means for more extensive instrumentation, particularly for
the determination and independent control of the sidewall and radial
heat transfer from the confined plasma. Significant improvements have
been effected in the design of the gas entry region including the nozzle
itself. The nozzle is of minimum length and two dimensional, thereby
providing a less turbulent jet with an optimum configuration for vortex
driving. Figure 1-1 illustrates the above-mentioned features.

The design of the water-cooled mixing chamber-nozzle will accommodate
injection of an alkali metal seed material into a region provided for
mixing the seed with the arc heated argon as well as improving the
uniform distribution of thermodynamic properties throughout the latter.
Seeding can be accomplished by injecting an aqueous solution of an alkali
metal, as was demonstrated previously, or by injecting the alkali metal
in a pure vapor or liquid form. The latter two methods offer the advan-
tages of helping to establish a plasma of relatively simple composition
which is free of oxidizing constituents. Furthermore, the electrical
conductivity is maximized because of the absence of poisoning constit-
uents, e.g., the electronegative hydroxyl radical.

3

FIGURE 1-1

ASSEMBLY DRAWING — VORTEX MHD GENERATOR

1. Duct One – Secondary Injection Port
2. Liquid Alkali Metal Feed Port
3. Water Discharge Port
4. Sidecover Gas Cooling
5. Tungsten Outer Electrode
6. Coolant Passage for Control of Radial and Electrode Heat Transfer
7. Powdered Zirconia Thermal Insulator
8. Armco Iron Side Cover
9. Zirconia Thermal Insulator
10. Magnesia Electrical Insulator
11. Tungsten Inner Electrode and Exhaust

12. Bosses for Arc Jet
13. Water Cooled Copper Mixing Chamber and Nozzle
14. Pressure and Thermocouple Instrumentation Port
15. Terminal for Outer Electrode
16. Stainless Steel Housing
17. Tungsten Terminal Strip

Various methods of vaporization and atomization of cesium and also potassium were considered. A boiler-superheater which was developed under AF33(616)7535 [1] has demonstrated adequacy and stability in the flow range of interest with potassium. It is expected that little or no alteration would be required for boiling and superheating cesium. However, because of the need to conserve the relatively expensive cesium and to expedite test sequences with the MHD generator, a system having a faster response to control was sought. This appears to be possible by metering the liquid metal directly to a gas-liquid atomizer from which the spray is subsequently directed into the jet issuing from the arc heater. Calculations [2] indicate that a diversion to the atomizer of ten per cent of the total argon flow is capable of producing droplet diameters of approximately 6 and 23 μ respectively for potassium and cesium. Subsequent vaporization in the arc heated argon takes place very rapidly - within a fraction of the length of the mixing chamber - according to a calculation procedure devised by Shapiro and Hawthorne [3]. Thus, equilibrium ionization is likely in the jets entering the cavity of the vortex generator.

The location of the jets with respect to a purely tangential entry into the vortex cavity was chosen on the basis of maximizing jet velocity recovery, considering the momentum loss [4] due to shear on the outer cylindrical surface. Thus, the effective vortex driving velocity was calculated to be 0.9 of the incoming jet velocity, for a radial Reynolds number $N_R = 66$ based on an effective eddy viscosity. The design of the generator, Figure 1-1, offers sufficient latitude in component design that relocation of the jets is easily accomplished should other arrangements appear more desirable.

Furthermore, nozzle expansion ratios may be altered most simply by changing the internal contours of that part of the nozzle which is actually integral with the outer electrode. The initial operation will attempt to achieve a jet Mach number of 0.75, an estimated optimum value for maximizing power output when the interrelationship between conductivity and velocity is considered with respect to power density.

Heat transfer in both the axial and radial direction was estimated for the generator. The estimate of radial heat transfer through the outer electrode was based on the application of Reynolds analogy of momentum and heat transfer to the momentum loss analysis of Rosenzweig [4]. The resulting radial heat transfer was 20 watt cm^{-2} for a stainless steel housing temperature of $1000°K$. An electrode temperature of $2600°K$ results thereby which will permit adequate thermionic emission of 1 amp cm^{-2} from a tungsten electrode.

Axial heat transfer from the generator sidewalls, estimated on the basis of the analysis [5] previously developed for this application, will be approximately 14 watts cm^{-2} for a housing temperature of $1000°K$. The resulting inner surface temperature of the magnesia electrical sidewall insulator will be approximately $1800°K$ and the magnesia-zirconia interface temperature $1700°K$. The latter two temperature levels should be satisfactory, both from the standpoint of negligible sidewall electrical shorting and the liquidus temperature ($1750°K$) of the magnesia-zirconia binary system.

The combined effects of all heat losses in the generator, but excluding those in the water cooled nozzles, results in a 4 per cent reduction of the plasma mean static temperature level. This, of course, has its consequences on the plasma conductivity.

The power conversion in the generator can be estimated conservatively on the basis of equilibrium plasma conductivity being maintained, allowing for the effects of heat transfer on the static plasma temperature distribution, and considering the effects of turbulence on the velocity distribution. The effective mean conductivity is approximately 1 mho cm^{-1} under the conditions of pressure, temperature, applied magnetic field of 1 weber m^{-2}, and relative cesium seed molar concentration of 0.015. An increase of 15 per cent in conductivity could be expected with a four-fold increase in concentration.[6] The gain, however, is certainly not warranted considering our present purposes and the relatively high cost of cesium.

The deviation from inviscid vortex flow can be judged with reference to Figure 5b of Reference 7 which indicates a measured velocity distribution of a vortex having similar non-dimensional flow and geometry parameters

with the exception of having a porous center body. The resulting conservative estimate of power is 860 watts, corresponding to an applied magnetic field of 1 weber m^{-2}.

A preliminary study of centerbodies for the vortex generator revealed that the desirability of tangential velocity stagnation, as effected completely by a porous center body, will depend upon the extent to which field induced nonequilibrium can elevate the conductivity in the region of the inner electrode. The best available information regarding nonequilibrium effects [8] suggest a simple nonstagnating exhaust electrode arrangement of the type illustrated in Figure 1-1 will perform best, in the case of a fairly shallow generator. Thus, the first electrode arrangement tried will be of this type.

2. Hydrodynamics of the Jet-Driven Vortex

Experimental Program. The first two phases of the cold-gas experimental study were completed in this quarter:

1) A preliminary visualization study of the flow in an incompressible vortex;

2) The design of a vortex chamber for detailed study of the velocity field in a compressible vortex.

Flow Visualization Study. In order to improve our physical intuition of vortex flow processes, and in an effort to explain seeming inconsistencies in the data of Reference 7, a flow-visualization study of an incompressible vortex was made. The flow of water in a single-nozzle vortex chamber was studied by means of flexible tufts, and by ink injection.

The dimensions of the vortex chamber, which was designed and used for an earlier study, were as follows: outside diameter, $D_o = 4$ inches; centerbody diameter, $D_i = 1, 2,$ or 3 inches; centerbody shape, tubular with five 0.030 inch wide circumferential slots; depth, $L = 0.375$ inch; nozzle width $W_j = 0.125$ inch; nozzle depth, $L_j = 0.375$ inch; nozzle location, outer surface tangent to outer wall of vortex, $D_j = 3.875$ inches. Thus, the pertinent dimensionless geometrical ratios were:

$$\frac{L}{D_o} = 0.0937$$

$$\frac{D_i}{D_o} = 0.25, \ 0.5, \ 0.75$$

$$\frac{D_j}{D_o} = 0.969$$

$$\frac{U}{V_j} = \frac{W_j}{\pi D_o} = 0.00995$$

For the flow-visualization study, the vortex chamber was equipped with fifty needles, each holding a tuft of black thread. All tufts were positioned in the midplane of the chamber.

8

Photographs of the tufts were taken for each of the three geometries at two turbulent radial Reynolds numbers: $Re = UD_1/2\nu \approx -400$ and -3000. A typical picture is shown in Figure 2-1. In addition, several pictures were taken at near-laminar Reynolds number, estimated to be $Re \approx -50$, with ink injection through the outer wall. The pictures were analyzed by measuring the angles assumed by the tufts, and by estimating the mean-flow streamline shapes.

At a given Reynolds number, the effect of the centerbodies was small; the tufts in the three pictures at either turbulent Reynolds number show identical flow directions. This is true of tufts both upstream and downstream of the centerbodies; these centerbodies certainly do not stagnate the tangential flow. There was some difference between the two turbulent flows for a given geometry; the flow at the lower Reynolds number was more radial, thus, the velocity recovery was poorer. All flows showed some angular dependence, which extended all the way in to the center body; this angular dependence was strongest near the nozzle, as expected.

The estimated mean flow streamlines show that a given "mean flow particle" will make two to three complete revolutions before reaching the one-inch centerbody, for the low Reynolds number case. At the high Reynolds number, at least one more revolution will result because of the higher tangential velocity recovery.

The near-laminar Reynolds number pictures show clearly that the slip plane between a laminar jet and a laminar vortex is unstable; this region immediately rolls up to form relatively small vortices which decay as the jet decelerates to the main vortex flow velocity. The disturbances which lead to the small vortices probably came from the needles which supported the tufts.

Vortex Chamber Design. At the conclusion of the hydrodynamic studies conducted under the preceding contract, definite recommendations, Reference 7, were made for the improvement of the existing experimental apparatus. These recommendations were to:

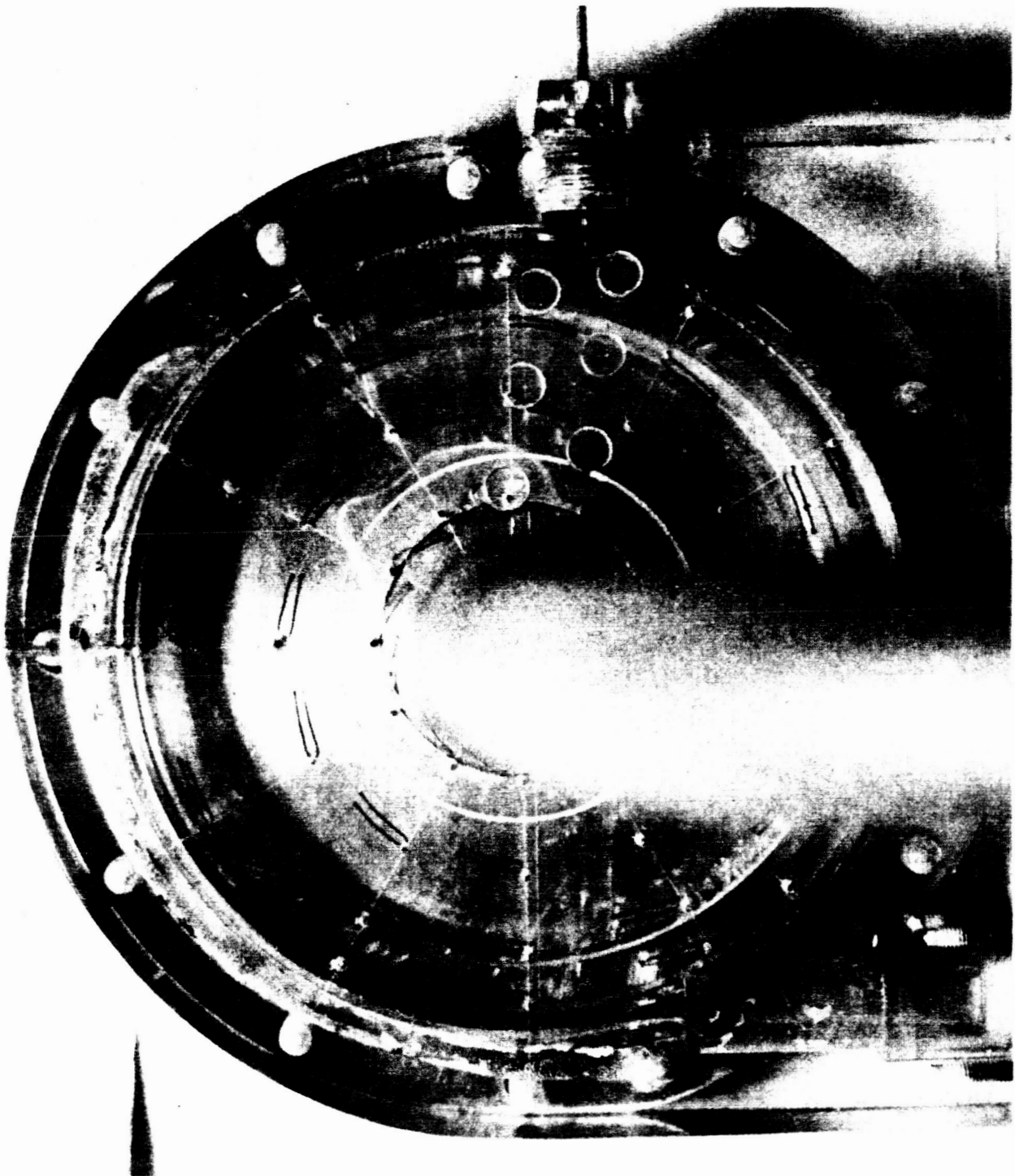> 1) Measure more accurately the mass flow rate of the air supplied to the vortex,

FIGURE 2-1

TUFT STUDY PHOTOGRAPH

2) Use larger settling chambers upstream of the nozzles, so that the inlet turbulence can be controlled,

3) Ascertain the effects of noncircular outer walls and nontangential driving jets,

4) Measure the total pressures in the vortex,

5) Measure the torques acting on various parts of the vortex chamber.

The first four of these improvements have all been incorporated into the newly-designed vortex chamber, and the fifth can be added easily if it seems desirable after preliminary testing.

The basic compressible vortex chamber model is shown in Figure 2-2. It consists of four nozzle blocks, which are bolted together to form the outer wall of the vortex chamber, and two side-wall plates, which contain the exit tubes and support the centerbody. The number of inlet nozzles can be changed by using one or more dummy nozzle blocks; the size or direction of the nozzles or the depth of the vortex chamber can be changed by using a different set of nozzle blocks. Changes in the exit tubes or centerbody are made by changing the side-wall plates. Thus the geometric design of the model is very flexible. The basic model will have the dimensions of the hot-gas test model, $D_o = 4$ inches, $D_i = 1.5$ inches, $L = 0.5$ inch, and $W_n = 0.25$ inch; additional tests will be run at other values of these variables.

The mass flow rate of the incoming air will be measured by means of an upstream pressure tap and a throat pressure tap in each nozzle. Thus, the flow rate through each nozzle can be independently measured and controlled. The nozzle design is such that the flow entering the vortex chamber is uniform and parallel, and since each nozzle is an independent unit, the incoming turbulence does not depend on the number of nozzles in use.

Figure 2-3 shows a traversing rig to be used for a variety of flow probes. This rig replaces one of the side-wall plates, and allows radial, axial, or tangential probing traverses; the probe can be located at any point in the vortex chamber, and rotated in the plane

FIGURE 2-2
VORTEX CHAMBER DESIGN

1. Nozzle Block
2. Side-wall Plate
3. Exit Tube
4. Clamping Screw
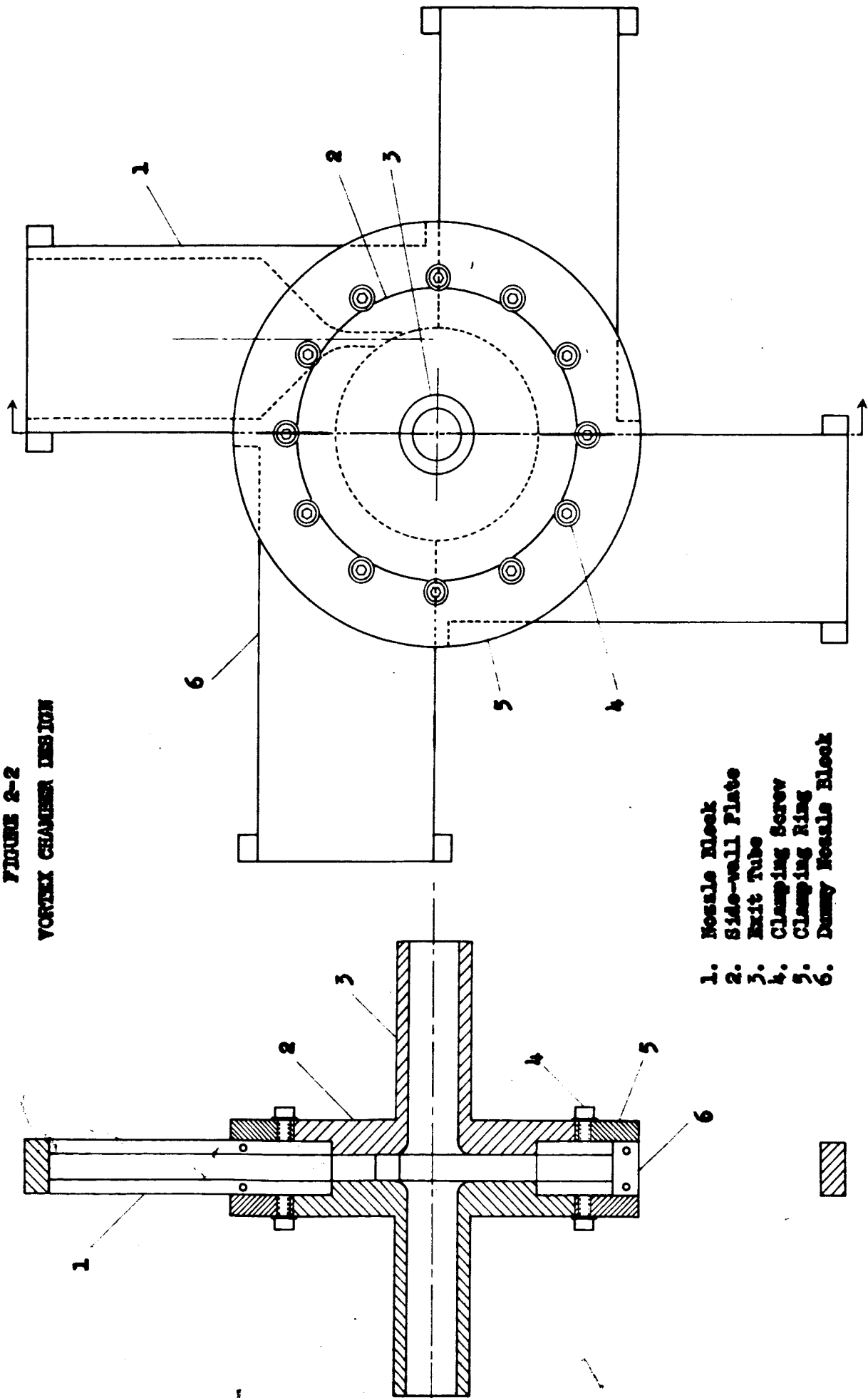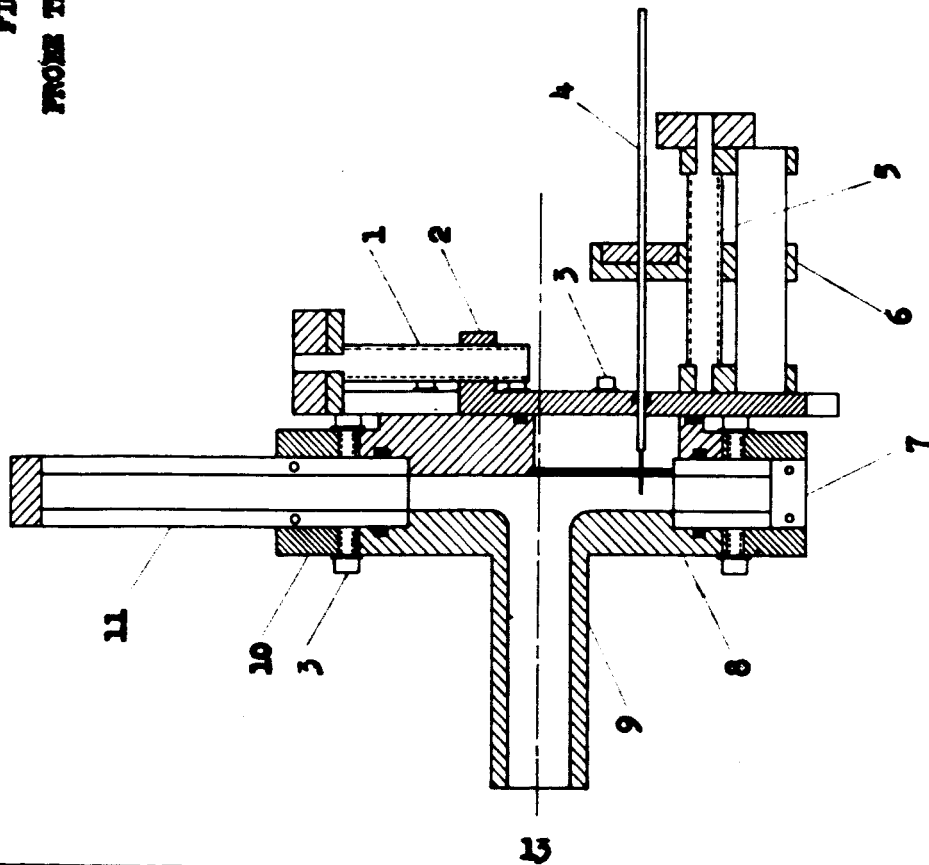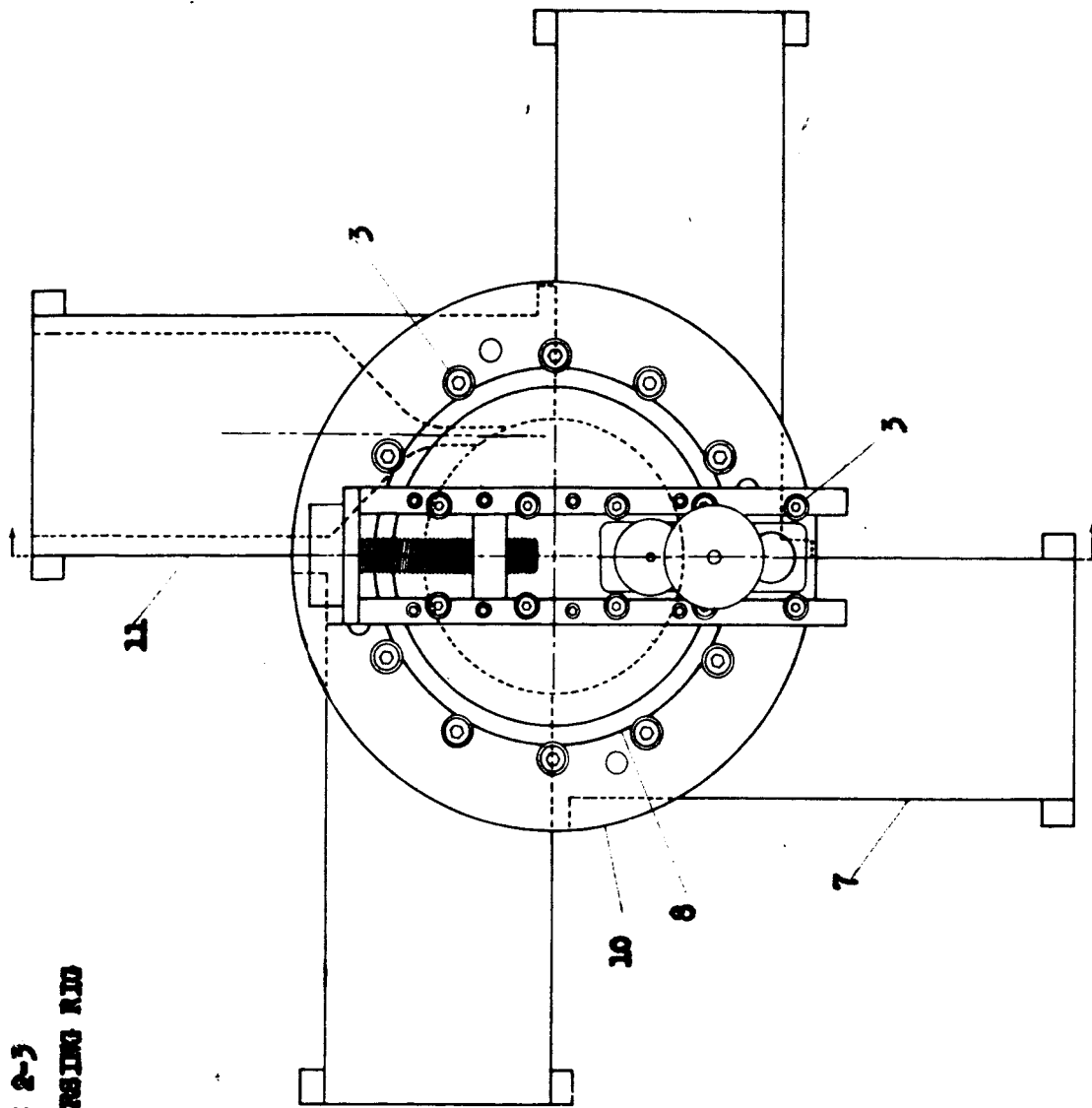5. Clamping Ring
6. Dummy Nozzle Block

12

FIGURE 2-3
PROBE TRAVERSING RIG

1. Radial Traverse Screw
2. Radial Traverse Slider
3. Clamping Screw
4. Probe
5. Axial Traverse Screw
6. Axial Traverse Slider
7. Dummy Nozzle Block
8. Side-wall Plate
9. Exit Tube
10. Clamping Ring
11. Nozzle Block

of the vortex to determine the flow direction. Probes which will be
used include a directional probe, allowing the flow direction and the
total pressure to be determined, a boundary layer probe, and a stag-
nation temperature probe. Future work may also make use of a hot-wire
probe if necessary.

Analytical Studies. Preliminary studies of incompressible vortex
flows have been based on the axisymmetric, constant eddy viscosity model.
The basic equations are, in plane polar coordinates,

(1) $\quad \rho \left(\dfrac{\bar{u}^2 + \bar{v}^2}{r} \right) = \dfrac{d\bar{p}}{dr}$

(2) $\quad \rho \left(\dfrac{d\bar{v}}{dr} + \dfrac{\bar{v}}{r} \right) = \varepsilon \dfrac{d}{dr} \left(\dfrac{d\bar{v}}{dr} + \dfrac{\bar{v}}{r} \right)$

(3) $\quad \dfrac{d\bar{u}}{dr} + \dfrac{\bar{u}}{r} = 0$

where
  $\bar{u}$ = mean radial speed
  $\bar{v}$ = mean circumferential speed
  $\bar{p}$ = mean static pressure
  ρ = fluid density
  ε = eddy viscosity
  r = radial coordinate measured from the axis of the vortex.

The problem governed by equations (1) - (3) is completed by specifying
a radial flow rate and inner and outer circumferential speeds. Consider
a radial through flow of

(4) $\quad Q = u_w r_w$

and circumferential speeds

(5) $\quad \begin{aligned} &\bar{v} = V_w \text{ at } r = r_w \\ &\bar{v} = V_1 \text{ at } r = r_1 \end{aligned}$

where r_w and r_1 are the outer wall radius and the inner wall radius,
respectively.

The solution to this problem is (see, e.g., Reference 4)

$$(6) \quad \bar{v} = Ar^{-1} + Br^{1} + Re$$

where the constants A and B are determined by (5) and

$$(7) \quad Re = \frac{\rho Q}{\varepsilon} = \frac{\rho u r}{\varepsilon}$$

Note that Re is negative for a radial flow from the outer to the inner region of the vortex.

Now the vortex flow represented by (6) is a good approximation to reality when there is no inner wall (which requires that $V_1 = 0$) and, of course, when the flow displays axial symmetry. It will, therefore, be employed to correlate the accurate data which will be obtained as described in the previous section. On the other hand, theoretical considerations suggest that the constant eddy viscosity model is also representative of the wall-remote* region of the flow in a vortex chamber having an inner porous wall. For this reason, it is felt that its consideration was abandoned prematurely during the early studies of last year's contract work (Reference 9).

One of the reasons the constant eddy viscosity model gave poor results in the past is that it was applied to a region of a vortex chamber which is characteristic of the inner (wall) region of a turbulent boundary layer. The proper way to apply this model is to assume that the velocity as given by (6) extrapolates to some non-zero velocity, V_1, at the wall. This outer profile is then matched to the inner profile which is governed by the so-called law of the wall. The matching is effected by requiring that the two profiles have a point of tangency where the eddy viscosity is equal. If this procedure is carried out, there results a unique value of wall friction for each choice of V_1. Clauser of Johns Hopkins did this in 1956 with gratifying results (Reference 10). His pseudo-laminar boundary layers, as he called them, gave excellent representations of the outer regions of turbulent boundary layers and an accurate wall friction law.

---

* The wall-remote region is that region where the ordinary viscous terms in the Navier Stokes equations are small compared with the turbulence terms.

Now equally good results should obtain for the wall-remote regions of a vortex chamber and preliminary calculations have been made to investigate this possibility. For this purpose arbitrary values of V_1 were chosen and the results are compared in Figure 2-4 with some data taken from Reference 7. Also shown is a theoretical curve of Reference 7 which was obtained by a numerical calculation.

One of the most curious results of the present preliminary study is that the data of Reference 7 for the case of small negative values of U/V_j (one and two jet configurations) can be approximated by the constant eddy viscosity model if a positive value of Re is employed. An example of this is shown in Figure 2-4 where data has been correlated by choosing Re = 0 and $V_1 = V_w$. Single driving jet data which are not shown have also been nicely approximated with the choice Re = +8. Now these results cannot possibly be consistent with physical reality and careful attention will be given to this point in future TRW studies. A probable reason for the inconsistency is that the one and two jet configurations of Reference 7 actually exhibit a strong profile variation in the circumferential directions.

Future analytical studies performed by TRW will be based on the constant eddy viscosity model as described above, for the wall-remote region. It should be noted that its use in no way contradicts the physical argument of Reference 9 which first led to the decision not to use it. As described above, and more fully in Reference 10, it does indeed represent a turbulent viscous flow if properly applied, i.e., matched to the inner wall region. One of the most important results the TRW effort is aimed at is a determination of the proper value of the eddy viscosity, ξ, to be employed in the mathematical model. Its value must depend strongly on the circumferential Reynolds number, N_v, according to physical considerations (see, e.g., Reference 11) of eddy sizes. This dependence of ξ on N_v is displayed by data presented in Reference 12. It also helps to explain the observed variation of profile shape with U/V_j at a constant value of N_u.
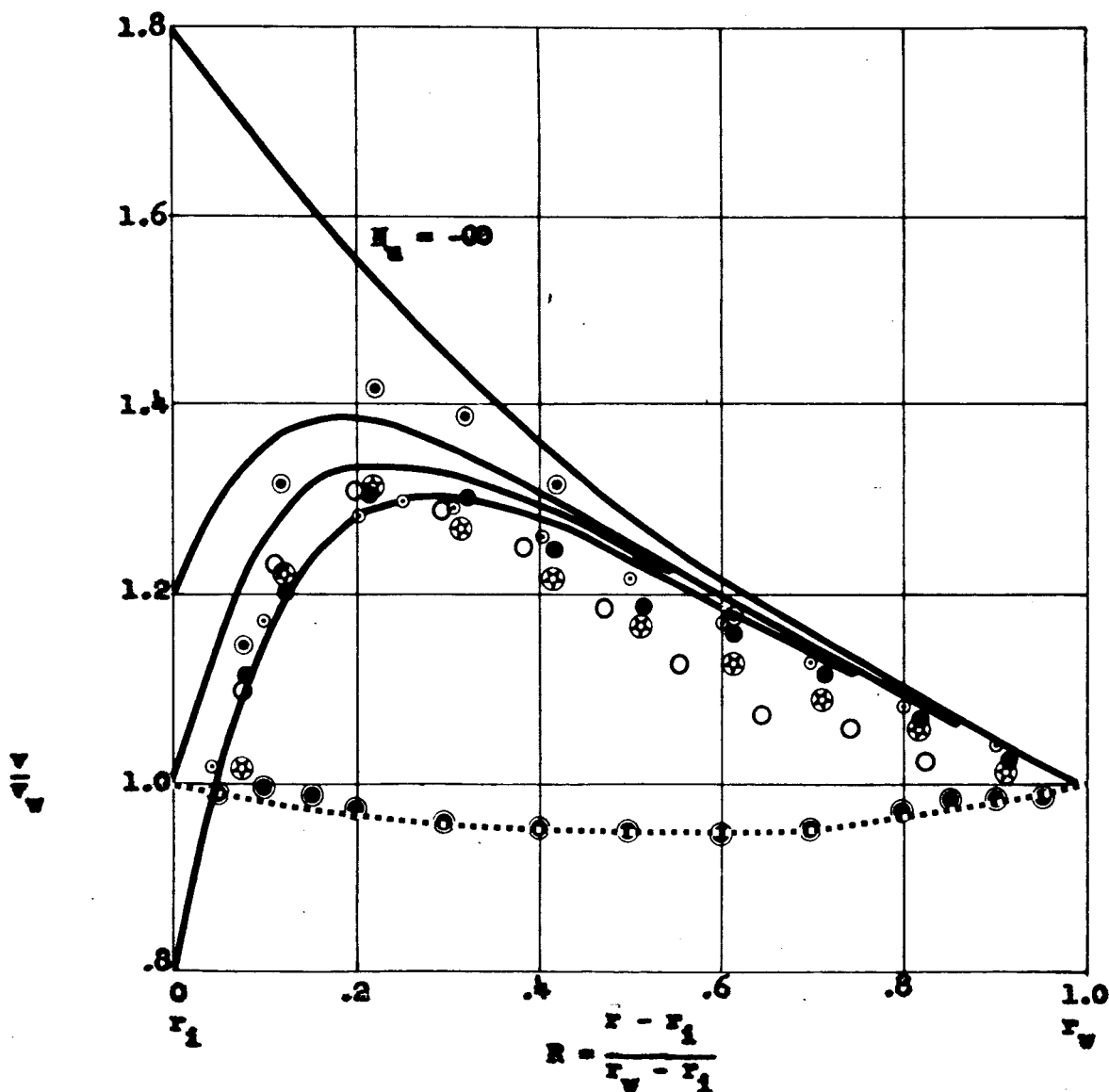
Comparison of Tangential
Velocity Profiles
Figure 2-4

IV   INTERPRETATION OF RESULTS AND CONCLUSIONS

The design of a new vortex MHD generator was completed along the lines
originally anticipated. The design appears capable of serving a wide
range of investigation with a minimum of change.

Flow visualization studies in an incompressible vortex revealed flow
behavior patterns which had been originally expected and reinforced
earlier conclusions that test procedures and analysis must recognize
the existence of nonuniformities in the azimuthal direction.

The design flexibility of the new vortex chamber for turbulence studies
will permit the acquisition of information pertaining to specific gener-
ator configurations as well as more general applications.

A pseudo-laminar boundary layer analysis was successfully applied to the
prediction of velocity profiles within a turbulent vortex. This new
approach promises to be more convenient than the application of mixing
length concepts originally suggested. However, further study will be
required to fully establish its range of applicability.

V   REFERENCES

1. L. I. Shure, "Heat Transfer Test Capsule Design Report",
    TRW TAPCO Report ER-4559, Sept. 1961.

2. J. J. Harmons, *Flow Properties of Disperse Systems*,
    Interscience Publishers, New York, New York, 1953.

3. H. W. Emmons (editor), *Fundamentals of Gas Dynamics*,
    Princeton University Press, 1958, p. 256.

4. M. L. Rosenzweig, "Velocity Recovery and Shear Reduction in Jet
    Driven Vortex Tubes", Aerospace Corp., Report No. TDR-594 (1203-01)TN-1
    March 1961.

5. S. Ostrach, "Estimate of Vortex Generator End-Plate Heat Transfer
    and Boundary - Layer Blockage Effects, TRW TAPCO Report ER-4426,
    May 1961.

6. B. W. Harned, et. al., "EM-731 Plasma Engine", WADD Technical Report
    60-895, Appendix I, January 1961.

7. G. G. Williamson and J. R. McCune, "A Preliminary Study of the
    Structure of Turbulent Vortices", ARAP Report No. 32, July 1961.

8. J. L. Kerrebrook, "Conduction of Gases with Elevated Electron
    Temperatures", *Engineering Aspects of Magnetohydrodynamics*,
    Columbia University Press, New York, 1962, pp. 327-346.

9. C. duP. Donaldson, "The Magnetohydrodynamic Vortex Power Generator:
    Basic Principles and Practical Problems", ARAP Report No. 30,
    March 1961.

10. F. H. Clauser, "The Turbulent Boundary Layer", *Advances in Applied
    Mechanics*, Vol. IX, 1956 Academic Press, p. 2 (and particularly
    Section IV, p. 34)

11. J. O. Hinze, *Turbulence*, McGraw-Hill, Sections 315 and 7.2, 1959.

12. J. J. Keyes, "An Experimental Study of Gas Dynamics in High Velocity
    Vortex Flow", *Proceedings of the 1960 Heat Transfer and Fluid Mechanics
    Institute*, Stanford University, p. 31.

National Aeronautics and Space Administration
1512 H Street, N.W.
Washington 25, D. C.
Attention: Walter Scott (P)   2 copies

National Aeronautics and Space Administration
1512 H Street, N.W.
Washington 25, D. C.
Attention: Herbert Hughes (RDP)

Ames Research Center
National Aeronautics and Space Administration
Moffett Field, California
Attention: Librarian

Goddard Space Flight Center
National Aeronautics and Space Administration
Greenbelt, Maryland
Attention: Librarian

Langley Research Center
National Aeronautics and Space Administration
Hampton, Virginia
Attention: Librarian

Lewis Research Center
National Aeronautics and Space Administration
21000 Brookpark Road
Cleveland 35, Ohio
Attention: Librarian   2 copies

Jet Propulsion Laboratory
National Aeronautics and Space Administration
Pasadena, California
Attention: Librarian

Marshall Space Flight Center
National Aeronautics and Space Administration
Huntsville, Alabama
Attention: Librarian

Manned Spacecraft Center
National Aeronautics and Space Administration
Houston, Texas
Attention: Librarian

Lewis Research Center
National Aeronautics and Space Administration
21000 Brookpark Road
Cleveland 5, Ohio
Attention: Henry O. Slone - SLPO

Lewis Research Center
National Aeronautics and Space Administration
21000 Brookpark Road
Cleveland 5, Ohio
Attention: John J. Fackler - SLPPO

Lewis Research Center
National Aeronautics and Space Administration
21000 Brookpark Road
Cleveland 5, Ohio
Attention: Bernard Lubarsky - SPU

Lewis Research Center
National Aeronautics and Space Administration
21000 Brookpark Road
Cleveland 5, Ohio
Attention: Norman T. Musial - Patent Counsel

Lewis Research Center
National Aeronautics and Space Administration
21000 Brookpark Road
Cleveland 5, Ohio
Attention: Richard Cave - SLPO

Lewis Research Center
National Aeronautics and Space Administration
21000 Brookpark Road
Cleveland 5, Ohio
Attention: John Weltmmy - APU

Lewis Research Center
National Aeronautics and Space Administration
21000 Brookpark Road
Cleveland 5, Ohio
Attention: Herman Schwartz - SEPO   2 copies (and a
                                                     reproducible copy)

Advanced Research Project Agency
Pentagon, Washington 25, D. C.
Attention: John Huth

Aeronautical Systems Division
Flight Accessories Laboratory
Wright-Patterson Air Force Base, Ohio
Attention: Donald Warnock

U. S. Air Force
Office of Scientific Research
Washington 25, D. C.
Attention: M. M. Slawsky

MHD Research
Newport Beach,
California
Attention: Donald Howard

U. S. Army Signal Research Development Laboratory
Fort Monmouth, New Jersey
Attention: Arthur Daniel

U. S. Atomic Energy Commission
Technical Reports Library
Washington 25, D. C.
Attention: J. M. O'Leary   3 copies

U. S. Atomic Energy Commission
Technical Information Service Extension
P. O. Box 62
Oak Ridge, Tennessee   3 copies

Institute for Defense Analysis
1825 Connecticut Avenue, N.W.
Washington 9, D. C.
Attention: Robert Hamilton

The Rand Corporation
1700 Main Street
Santa Monica, California
Attention: Librarian

Airesearch Manufacturing Division
The Garrett Corporation
Phoenix, Arizona
Attention: Librarian

Allison Division
General Motors Corporation
Indianapolis 6, Indiana
Attention: Librarian

Electro-Optical Systems Inc.
125 N. Vinedo Avenue
Pasadena, California
Attention: Joseph Goustein

General Electric Company
Missile and Space Vehicle Division
Valley Forge, Pennsylvania
Attention: George W. Sutton